Article

Not peer-reviewed version

# Comprehensive Evaluation Of Wet Spun Polyhydroxyalkanoate Fibres: Morphology, Crystallinity, And Thermal Properties

Marta A. Teixeira * , Inês Leite , Raquel Gonçalves , Helena Vilaça , Catarina Guise , Carla Silva

Posted Date: 2 July 2025

doi: 10.20944/preprints202507.0116.v1

Keywords: polyhydroxyalkanoates; biodegradable polymers; wet spinning; fibre morphology; thermal properties; mechanical properties; sustainability

 doi:10.20944/preprints202507.0116.v1



*Article*

# Comprehensive Evaluation Of Wet Spun Polyhydroxyalkanoate Fibres: Morphology, Crystallinity, And Thermal Properties

**Marta A. Teixeira *, Inês Leite, Raquel Gonçalves, Helena Vilaça, Catarina Guise and Carla Silva**

CITEVE-Technological Centre for the Textile and Clothing Industries of Portugal, Vila Nova de Famalicão, Portugal

* Correspondence: mteixeira@citeve.pt

**Abstract**

In response to the increasing environmental concerns, significant efforts have been made to reduce the reliance on fossil fuel-based plastics, driving the development of sustainable alternatives such as polyhydroxyalkanoates (PHAs). This study investigates the processing of various PHAs into fibres, focusing on their morphological, thermal, and mechanical properties. Different PHAs were spun into fibres at a 15% (w/v) concentration using wet spinning techniques. Among the PHAs studied, commercially available PHBHHx, used as a reference, exhibited a spongy morphology in the fibres and demonstrated thermal vulnerability due to its rapid degradation. Blended fibres showed enhanced morphological and mechanical properties compared to neat fibres. In Fourier-transform infrared spectroscopy (FTIR), no differences were observed between the unprocessed polymers and the wet spun polymeric fibres, indicating that the wet spinning process did not affect the molecular structure of the polymers. Thermal and mechanical evaluations confirmed the miscibility between the polymers in the blends. Overall, these results highlight the potential of polymer blending to enhance fibre functionality and broaden their application potential. However, the study also emphasizes the need to explore optimized feed rates to improve fibre production efficiency and increase their resistance, to enlarge their suitability for various applications.

**Keywords:** polyhydroxyalkanoates; biodegradable polymers; wet spinning; fibre morphology; thermal properties; mechanical properties; sustainability

## 1. Introduction

Owed to the excellent properties of plastics, such as high versatility, high strength-to-weight ratio, low weight, resistance to physical and chemical degradation and low cost, they can be found in various sectors [1]. Packaging, construction, textiles, electronics, transportation, food, healthcare, and energy are just some examples of the industries widely using plastics [2]. However, increased environmental awareness has led to the reduction and replacement of fossil fuel plastics, which has consequently contributed to the development of bioplastics [3]. It is estimated that the global bioplastic market size will grow at 24.2% till 2029, when it will reach USD 45.2 billion (from USD 27.84 billion in 2025). Regarding the bioplastic' European market, it is expected to expand at a compound annual growth rate of 18.3% up to 2030 [4]. Bioplastics can be defined as plastics that i) are made from renewable resources ('bio-based'), ii) are biodegradable, iii) are made through biological processes, or iv) a combination of these [5]. These bioplastics have various benefits over petroleum-based plastics, including a lower carbon footprint, energetic efficiency, biodegradability, and might have improved material properties. Nonetheless, bioplastics often exhibit lesser properties such as thermal instability, low melt strength and poor processability that can limit their application [6]. In addition, their cost, production scale, recyclability, and legislation are some current challenges

 doi:10.20944/preprints202507.0116.v1



that bioplastics still face [7]. The most widely used bioplastics in the global market comprise non-biodegradable polymers such as, polyethylene (bio-PE), polyethylene terephthalate (bio-PET), polypropylene (bio-PP), and biodegradable polymers, including polybutylene succinate (PBS), polybutylene adipate terephthalate (PBAT), polylactic acid (PLA), thermoplastic starch and polyhydroxyalkanoates (PHAs) [8,9]. Among these bioplastics, polymers from the PHAs group have attracted significant attention as alternatives to petroleum-based plastics [10]. PHAs have important advantages, such as their production by biogenesis from different sources (renewable energy sources, production waste, fossil sources and organic acids) using different types of bacteria, as well as having superior biodegradability compared to other polymers [11]. PHAs are linear aliphatic polyesters, composed of monomeric units of R-hydroxyalkanoic acids. More than 150 different PHAs monomers have been identified, contributing to a materials group with tuneable characteristics in terms of mechanical properties and degradation rates [12,13]. A vast variation in the length and composition of the side chain of PHAs has been described and their molecular weights have been found within the range of 50,000 to 1,000,000 Da [14]. Based on the monomer structures, PHAs are divided into short chain length (scl), medium chain length (mcl) and long-chain length (lcl). The formers consisting of C3-C5 hydroxyl fatty acids such as 3-hydroxybutyrate (3HB), 3-hydroxypropionate (3HP), 4-hydroxybutyrate (4HB), and 3-hydroxyvalerate (3HV), the mcl containing C6-C14 hydroxyl fatty acids typically including 3-hydroxyhexanoate (3HHx), 3-hydro-xyheptanoate (3HHp) to 3-hydroxytetradecanoate (3HTD), and the lcl having more than C14 in their chain, e.g., 3-hydroxyhexadecanoate and 3-hydroxypentadecanoate [15,16]. Although poly(3-hydroxybutyrate) (P3HB) is the most widely studied PHA, its use at industrial scale is limited due to some drawbacks, such as its relatively narrow processing window as its thermal degradation occurs at temperatures only slightly higher to the melt temperature. On the other hand, P3HB presents high stiffness which results in a high fragile polymer due to its recognized high crystallinity [17–19]. By adjusting the composition of the monomers, PHAs with improved thermal and mechanical properties can be obtained. The incorporation of mcl monomers into P3HB has resulted in the production of commercially attractive copolymers since these combine the strength of P3HB and the flexibility of mcl PHAs [20]. So far, random copolymers including poly(3-hydroxybutyrate-co-3-poly-hydroxyvalerate) (PHBV), poly(3-hydroxybutyrate-co-4-hydro-xybutyrate) (P3HB4HB), and poly(3-hydroxybutyrate-co-3-poly-hydroxyhexanoate) (PHBHHx) have been found to exhibit advantageous thermal and mechanical properties, although they still suffer from property detrimental aging effects [15,21,22]. In addition to these structural changes to PHAs, the investigation of new processing techniques is important to further expand the potential application of these biopolymers [7].

The processing of PHAs into fibres can be a beneficial strategy to create and design more suitable applications and to add specific functional properties [23]. Wet spinning is an industrialized fibre producing technique, which involves the injection of a polymeric solution into a coagulation bath composed of a non-solvent or a poor solvent of that polymer. It results in a fast precipitation of the polymer, as well as a solvent removal, and coagulant penetration, forming solid microfibers [24,25]. This technique, comparatively to the melt spinning, allows low processing temperatures, being a preferable method for the processing of PHAs to avoid their thermal degradation [26]. Production of PHAs wet spun fibres, such as P3HB [27], poly-4-hydroxybutyrate (P4HB) [28], PHBV [29,30], PHBHHx [7,31], poly(3- hydroxybutyrate-co-4-hydroxybutyrate) (P3HB4HB) [32] and blends thereof [33] have already been reported in the literature. The produced wet spun fibres are characterized by presenting high porosities, different dimensions, wide rays of organizations and physical and chemical properties [34,35].

In this study wet spun fibres were developed from newly developed and partially synthesized PHAs. The primary objective was to identify the proper conditions for the dissolution and coagulation and to assess the properties of the produced fibres. To this effect, a comprehensive physicochemical characterization was conducted on both neat and blended fibres using scanning electron microscopy (SEM), Fourier transform infrared spectroscopy with attenuated total reflectance

 doi:10.20944/preprints202507.0116.v1



(FTIR-ATR), thermogravimetric analysis (TGA), differential scanning calorimetry (DSC), and stress-strain testing.

## 2. Materials and Methods

### *2.1. Materials and Reagents*

PHBHHx powder was purchased from Bluepha (Beijing, China) and partially synthe-sized P3HBs (PHA.C.3.3.1.4 and PHA.A.2.3.1.1) in granules form were kindly provided by the University of Kaiserslautern (Germany). The weight average molecular weight (Mw) and the polydispersity (PD) expressed by the ratio of Mw/Mn (where Mn means number average molecular weight) of each polymer are shown on Table 1. Glacial acetic acid, chloroform and ethanol were obtained from Fisher Scientific™, while calcium chloride was purchased from Carlo Erba Reagents. Plastic luer lock syringes of 5 mL and 21G needles with, bevelled tips with dimensions of 0.80*40 mm were acquired from VWR. All reagents were used without further purification.

**Table 1.** Characteristics of the raw materials.

| Polymer | Mw (Da) | Mw/Mn |
|---|---|---|
| PHBHHx | 291000 | 4.51 |
| PHA.A.2.3.1.1 | 256423 | 3.30 |
| PHA.C.3.3.1.4 | 215659 | 2.10 |

### *2.2. Study On Processing Parameters of The Wet Spinning Technique*

Concentrations of 10%, 15%, and 20% (w/v) were selected to evaluate the solubility of each PHA in chloroform. The boiling point of chloroform (61.2 °C) was considered to prevent complete solvent evaporation during the dissolution process [36,37]. PHBHHx powder and PHA granules were mixed with chloroform and heated to its boiling point in a covered beaker under continuous stirring. The mixtures were maintained under these conditions until complete dissolution of the respective PHAs was achieved.

To identify the optimal coagulation bath conditions, drop tests were conducted in various baths. The coagulation baths tested included water (at temperatures ranging from cold to hot), ethanol, acetone, propanol, methanol, sodium hydroxide, ethyl acetate, and hexanol. During the drop tests, polymer solutions were added dropwise to the potential coagulation baths in glass vials, and tweezers were used to stretch the polymer drop during coagulation.

### *2.3. Production of Wet Spun PHA Fibres*

Polymeric solutions of the different PHAs were prepared at 15% (w/v) in 100% chloroform. These solutions were continuously stirred at room temperature (RT) for 2 h. Each polymer was wet spun firstly individually to produce neat fibres, and later in blends, which consisted of 70/30 % (v/v) of PHA.C.3.3.1.4/PHBHHx and PHA.C.3.3.1.4/PHA.A.2.3.1.1 15% (w/v) solutions in 100% chloroform, respectively.

All PHAs solutions were extruded at 0.07 mL/min into an ethanolic coagulation bath at RT. Spun fibres were submerged into the coagulation bath before being pulled out and collected manually (using tweezers), dried for 24 h at RT and washed for 5 min in dH2O for removal of some coagulation bath and solvent. After production, the fibres were stored in a desiccator.

To ensure clear identification, the powder, and granules PHAs will be referred to as unprocessed PHAs from now on. Fibres produced from 100% of each PHA will be labelled as neat fibres. When necessary, the fibres will be specifically identified by the PHA from which they originated.

 doi:10.20944/preprints202507.0116.v1



*2.4. Morphological Analyses*

Morphological analyses of the fibres produced were performed on a scanning electron microscopy (Zeiss Evo 10) at an acceleration of 20 kV. Fibres were initially coated with a thin layer of Au using a BIO-RAD SC502 sputter coater. The average of fibres diameters was determined by conducting 100 measurements on three micrographs. Images at a magnitude of 500× were used and processed using the ImageJ® software (version 1.44, National Institutes of Health, USA).

*2.5. Chemical Analysis*

A Spectrum One, Perkin Elmer spectrophotometer with a diamond crystal was used. Each spectrum was obtained in transmittance mode, by accumulation of 45 scans with a resolution of 4 $cm^{-1}$ in the range of 400 to 4000 $cm^{-1}$. Spectra were collected in triplicate.

*2.6. Thermal Analysis*

Thermal degradation behaviour was assessed by weight loss monitoring with a temperature increase in the range of 30-700 °C, at a heating rate of 20 °C/min under synthetic air atmosphere and flow rate of 40 mL/min on a TGA 209 F1 Libra by Netzsch, using alumina pans. Results were plotted as the percentage of weight loss vs. temperature. Differential thermogravimetric (DTG) analysis was additionally conducted to identify the ranges of temperature at which the most significant degradation peaks were registered.

Thermal properties of unprocessed PHAs and fibres were also evaluated using a Mettler Toledo DSC 3+. Samples were submitted to two heating cycles: the first heating step from -40 to 200 °C at 5 °C/min, followed by holding at 200 °C for 3 minutes before cooling to -40 °C at 5 °C/min. Samples were reheated to 200 °C with the same heating rate. All tests were performed under a dynamic nitrogen atmosphere.

*2.7. Mechanical Analyses*

The fibres were tested for their linear mass, tensile strength, elongation, and tenacity by the vibroscope method according to EN ISO 1973:2021+EN ISO 5079:2020 and their lengths were determined according to NP 1874:1982 using a Favigraph from Textechno Herbert Stein GmbH & Co. KG (Monchengladbach, Germany). The tests were conducted at a clamping length of 10 mm and 5 mm/min test speed. The pre-load weight needed to stretch the fibres according to the linear density was 100 mg. Twenty-five measurements were conducted for each sample.

## 3. Results and Discussion

*3.1. Optimization of the PHA Fibre Production Process*

In the wet spinning technique, factors such as the type of solvent used, the type and conditions of the coagulation bath, the concentration of the solution, and the spinning rate all play a major role in determining the morphology, molecular alignment, and mechanical properties of the resulting fibres [38,39].

Among the solvents used, chloroform was the most suitable to fully dissolve the PHAs in all concentrations tested in a faster rate of dissolution. Chloroform was also the only solvent that enabled fibre production from ethanolic coagulation baths. Ethanol was also the coagulation bath most efficient between those tested. It was also determined that among the various polymer concentrations tested, 15% (w/v) was the most suitable. The concentrations of 10% and 20% (w/v) did not permit an effective fibre production for all polymer types. and therefore, these concentrations were excluded from the comparative analysis. In some cases, 20% (w/v) of different PHAs caused needle clogging. Additionally, the 10% (w/v) PHAs fibres produced showed to be very fragile and difficult to remove from the coagulation bath. Due to its viability and structural integrity after the collection process,

 doi:10.20944/preprints202507.0116.v1



only the 15% (w/v) concentration was selected to produce all fibres. Therefore, all results presented are relative to this concentration.

A proper coagulation rate is crucial for producing fibres with structural integrity [40]. Therefore, identifying the right combination of processing parameters is essential to form stretchable polymeric fibres. This study found that PHA solutions prepared in chloroform and extruded into an ethanol-based coagulation bath at a flow rate of 0.07 mL/min successfully produced wet spun fibres from all PHAs studied and their blends.

### *3.2. Morphological and Diameter Analysis of the PHA-Produced Fibres*

SEM micrographs and fibre diameters are presented in Figure 1. High-magnification micrographs of the produced fibres reveal distinct morphological and shape differences. A spongy morphology was observed exclusively in neat PHBHHx fibres (Figure 1A). This morphological characteristic in PHBHHx wet spun fibres was previously reported by Puppi et al. [35] and Mota et al. [41]. This effect has been attributed to solvent/non-solvent counter-diffusion during polymer solution coagulation, leading to phase separation into a polymer-rich and a polymer-poor phases [25,38,41]. The spongy effects have been identified as beneficial features, as they positively influence the biodegradation rate [35].

Neat PHA.A.2.3.1.1 (Figure 1B) and PHA.C.3.3.1.4 (Figure 1C) fibres, despite showing some surface irregularities and not being entirely smooth, did not exhibit polymer-poor phases like the spongy effect observed in neat PHBHHx fibres. Among the individual fibres, the neat PHA.C.3.3.1.4 fibres exhibited a more uniform and rounded geometry. The average fibre diameters, summarized in Figure 2, were determined by randomly measuring 50 points on each fibre. The calculated average diameters for neat PHBHHx, PHA.A.2.3.1.1, and PHA.C.3.3.1.4 fibres were 65.54 ± 7.34 μm, 164.98 ± 18.12 μm, and 84.88 ± 11.05 μm, respectively. As shown, the fibres produced from the commercial polymer PHBHHx exhibited the smallest diameters. Similar diameter values for PHBHHx fibres, ranging between 47–76 μm, were also reported by Puppi et al. and Mota et al. [38,41]. Among both PHA.C.3.3.1.4 and PHA.A.2.3.1.1 fibres, the former also exhibit smaller diameters.

For the blended fibres (Figure 1D,E), the combination of PHAs enhanced fibre geometry and reduced diameter, resulting in more rounded and thinner fibres, compared to the neat ones. Moreover, the blended fibres exhibited greater uniformity in diameter, as reflected by the smaller standard deviation values from the diameter measurements. These benefits of blended polymeric fibres can be attributed to improved spinnability and favourable phase interactions between the PHAs, which facilitate better packing and enhance stretching and thinning during spinning. Additionally, the presence of different polymers has been reported to influence solvent evaporation and polymer coagulation processes, often leading to tighter packing and smaller diameters [42,43].

In that regard, PHA.C.3.3.1.4/PHBHHx blended fibres displayed the most uniform cylindrical shape (Figure 1D), a result further supported by the smallest standard deviation values observed among all fibres (Figure 2). Notably, these fibres despite having PHBHHX on their composition did not present a spongy structure as observed on neat PHBHHx fibres. This absence of the spongy morphology may be attributed to the higher concentration of PHA.C.3.3.1.4, which likely mitigates the phase separation typically induced during the coagulation process by the presence of PHBHHx. In terms of diameter analysis, the PHA.C.3.3.1.4/PHBHHx fibres exhibited the smallest diameters amongst all fibres produced, measuring approximately 31.46 ± 4.22 μm. PHA.C.3.3.1.4/PHA.A.2.3.1.1 blended fibres also displayed low diameters of approximately 37.48 ± 4.66 μm. These data shows that PHA.C.3.3.1.4 exhibits excellent blending and packing capabilities with the other polymers used, enhancing their spinnability and, consequently, their final morphological properties.

 doi:10.20944/preprints202507.0116.v1



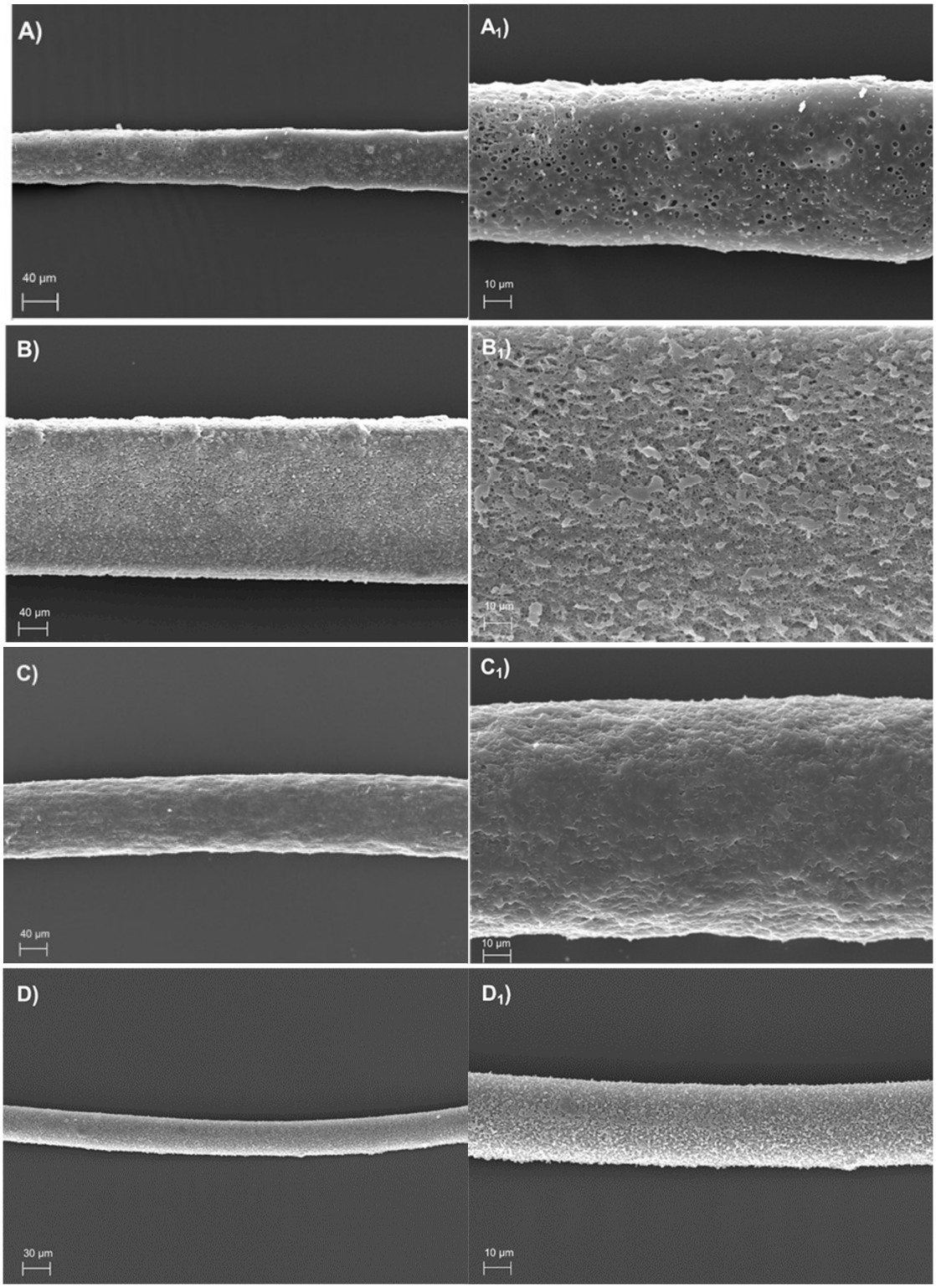

 doi:10.20944/preprints202507.0116.v1



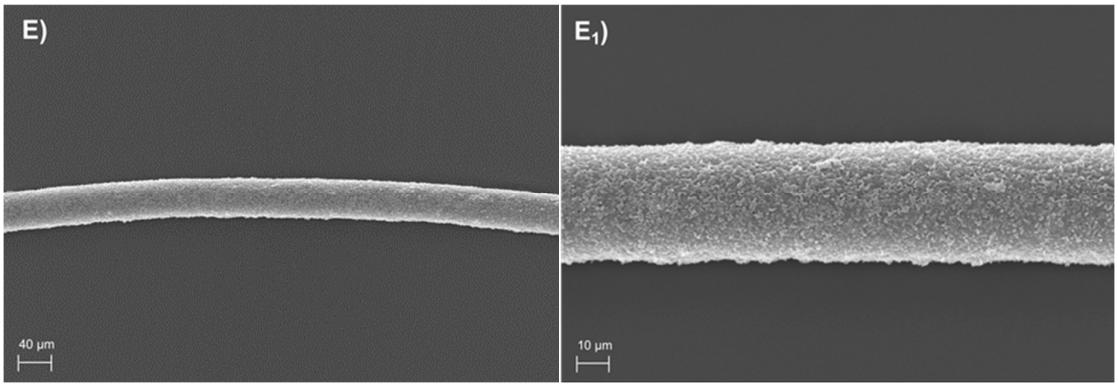


**Figure 1.** SEM micrographs of the wet spun fibres produced: PHBHHX (A), PHA.A.2.3.1.1 (B), PHA.C.3.3.1.4 (C), PHA.C.3.3.1.4 / PHBHHX (D) and PHA.C.3.3.1.4 / PHA.A.2.3.1.1 (E). All left micrographs are shown with a magnification of 500×, while all right micrographs present a magnification of 1500×.

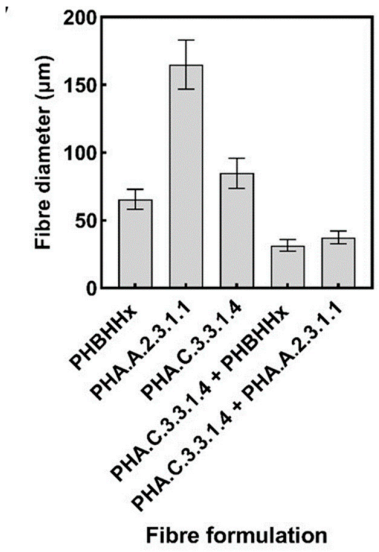


**Figure 2.** The Kruskal-Wallis test was used, with multiple comparisons between different fibre formulations, to determine the statistical significance of the diameter distribution of the different PHA wet spun fibres. A p-value < 0.001 was observed for all formulations (see supporting information).

*3.3. Chemical Analysis*

Distinct absorption peaks were observed in similar regions of the FTIR spectra of both unprocessed PHA and their fibres (Figure 3). A prominent absorption band at 1720 $cm^{-1}$ corresponds to the carbonyl (C=O) stretching of the ester group, while another band at 1276 $cm^{-1}$ is attributed to the -CH group [44,45]. These bands are commonly recognized as characteristic markers for PHA. Additionally, a series of bands between 1000 and 1300 $cm^{-1}$ represent the stretching of the C-O bond in the ester group. The bands at 2981 and 2928 $cm^{-1}$ signify the presence of methyl ($CH_3$) and methylene ($CH_2$) asymmetric and symmetric stretching modes, respectively [46].

No differences were observed between the FTIR spectra of unprocessed PHAs and their wet spun fibres, indicating that the polymer molecular structure was not affected by the wet spinning process.

 doi:10.20944/preprints202507.0116.v1



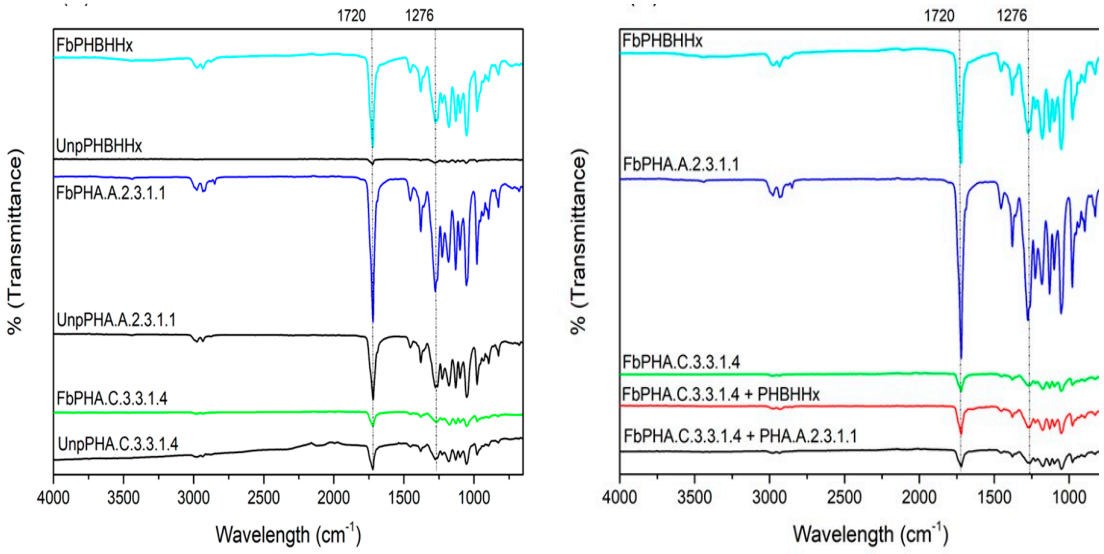


**Figure 3.** ATR-FTIR characterization of the PHAs, between unprocessed and PHA fibres (a) and between only the fibres produced (b).

*3.4. Thermal Characterization*

TGA and DSC analyses were conducted to assess the thermal stability and structural characteristics of both the unprocessed polymers and their wet spun fibres.

In this context, Figure 4A,B display the TGA and DTG thermograms, respectively, of the unprocessed polymers (UnpPHAs) and the produced fibres (FbPHAs). Table 2 presents the main degradation events of TGA, as well as glass transition temperature ($T_g$), melting temperature ($T_m$), and level crystallinity ($X_c$) from second heating scans.

TGA evaluations revealed that the unprocessed PHAs exhibited higher degradation temperatures and lower mass loss compared to the produced fibres (Table 2). This is likely due to their more compact molecular structure and higher crystallinity [47]. Among the unprocessed polymers evaluated, PHBHHx (the commercial polymer) was found to be the most thermally vulnerable. Its degradation step occurs fastest, and starts from almost 260 °C, being complete at approximately 284 °C. These values are also aligned with the low $T_m$ and $X_c$ determined for unprocessed polymer PHBHHX, as shown in Table 2. These thermal structural features are consistent with some studies already carried out [48–50]. The thermal degradation behaviour of PHBHHx has been characterized by the formation of shorter chain fragments with carboxylic terminal groups. Crotonic acid is produced as a by-product through a random chain scission mechanism [51]. In contrast, the partially synthesized P3HB polymers used, such as PHA.A.2.3.1.1 and PHA.C.3.3.1.4, exhibited higher thermal resistance. These unprocessed polymers displayed the highest onset and maximum degradation temperatures, as easily seen in Figure 4. These features may be attributed to the renowned high crystallinity of PH3B [52,53]. Among the unprocessed polymers, PHA.A.2.3.1.1 demonstrated the highest $X_c$. In contrast, PHA.C.3.3.1.4 exhibited the lowest $T_g$ and $X_c$, suggesting it holds the most flexible chains or smaller side groups [54]. However, its high $T_m$ may indicate stronger bonding between its chains, a result clearly reflected in its outstanding elongation capacity observed during mechanical analysis [55].

Regarding the fibres produced, their thermal stability is lower compared to the unprocessed polymers which may occur due to increased amorphousness, processing-induced defects, and the presence of solvents [56,57]. These effects may have also arisen due to the low feed rate used during the extrusion. It may have contributed to an incomplete polymer chain alignment, leading to a higher mass loss during degradation, ranging from 97% to 100%. According to the literature, a faster rate of

 doi:10.20944/preprints202507.0116.v1



coagulation quickly forms a 'skin', followed by the coagulation of the core. This process creates an oriented fibrous structure, which enhances the thermal properties of the fibres [58,59]. By this reason, wet spun fibres typically demonstrate higher crystallinity compared to their corresponding polymeric granules due to molecular alignment during spinning [60,61]. However, the highest $T_m$ values were observed on fibres, suggesting that the bonds established during extrusion were stronger than those on unprocessed PHAs.

Notably, evidence of excellent miscibility between the polymers was observed in the blended fibres, as indicated by the presence of a single maximum degradation temperature and $T_m$. The blended fibres composed of PHA.C.3.3.1.4/PHA.A.2.3.1.1 exhibited the highest crystallinity values. This, coupled with the recorded $T_m$ values, underscores the exceptional ability of these polymers to achieve efficient chain blending and alignment. This data is aligned with the lowest diameters and roundest shape obtained on these blended fibres.

**Table 2.** Data relevant to thermal characterization by DSC and TGA analysis (n = 3; S.D. < 1%).

| | | *$T_{onset}$ (°C) | [a]$T_{Max}$ (°C) | % Mass Loss | $T_g$ (ºC) | $T_m$ (ºC) | $X_c$ (%) |
|---|---|---|---|---|---|---|---|
| **Unprocessed polymers** | PHBHHX | 263.4 | 275.7 | 2.80 | -3,44 | 103.3/119.9 | 24.9 |
| | PHA.A.2.3.1.1 | 286.8 | 297.8 | 6.20 | | 135.8/157.6 | 42.9 |
| | PHA.C.3.3.1.4 | 288.2 | 300.4 | 4.60 | -24,8 | 167.2 | 19.7 |
| **Fibres** | PHBHHX | 240.1 | 270.0 | 97.46 | - | 110.8/130.6 | 10.9 |
| | PHA.A.2.3.1.1 | 252.3 | 272.0 | 100.71 | - | 162.6 | 25.1 |
| | PHA.C.3.3.1.4 | 267.3 | 292.0 | 98.71 | - | 171.1 | 25.0 |
| | PHA.C.3.3.1.4 / PHBHHX | 248.3 | 274.0 | 100.28 | - | 158.3 | 11.0 |
| | PHA.C.3.3.1.4 / PHA.A.2.3.1.1 | 243.4 | 272.0 | 98.06 | - | 166.6 | 46.4 |
| | PHBHHX | 240.1 | 270.0 | 97.46 | - | 110.8/130.6 | 10.9 |

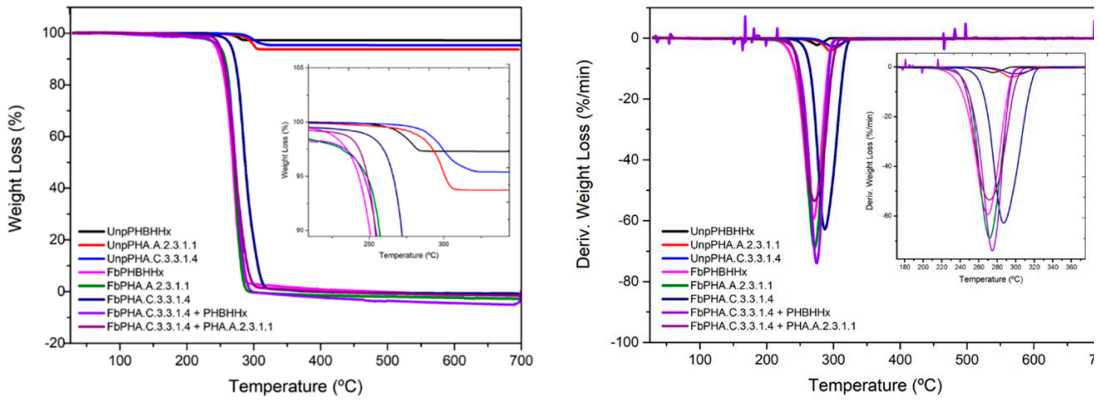


(**a**) (**b**)

**Figure 4.** TGA thermograms showing weight loss (a) and derivative weight loss (b) profiles of the unprocessed PHAs (UnpPHAs) and PHAs fibres (FbPHAs).

 doi:10.20944/preprints202507.0116.v1



*3.5. Mechanical Properties of the PHAs-Produced Fibres*

The mechanical testing results presented in Table 3 were analysed in terms of linear mass, tenacity, and elongation at break for all five types of fibres. Notably, the neat PHA.A.2.3.1.1 and PHC.3.1.1.4 fibres exhibited the highest linear mass. Although all fibres were produced under identical technical conditions, these polymers demonstrated higher swelling of their extruded polymeric chains as they exited the needle. These values surpass those reported by Singhi et al. in their development of wet spun PH4B fibres [28].

In contrast, the blended fibres exhibited a lower linear mass compared to the neat fibres. This observation aligns with the findings from morphological and diameter analyses, which revealed that the blended fibres were thinner and more uniformly rounded.

The tenacity values of all the fibres were similar and notably low. This could be attributed to the low feed rates used during the extrusion process. Insufficient feed rates may disrupt the consistency of polymer flow, resulting in incomplete coagulation and improper alignment of the polymer chains [62,63]. These factors led to fibres with reduced tenacity.

Among all the fibres tested, the neat PHA.C. 3.3.1.4 demonstrated the highest elongation at break, reaching around 136%. This exceptional elongation can be attributed to the enhanced polymer chain entanglements [64]. Additionally, this high elongation value aligns with the high $T_m$ values and low crystallinity observed in its DSC curves, as shown in Table 2. It is well-documented in the literature that polymers with lower crystallinity typically exhibit higher elongation at break [65]. This condition is also supported by the mechanical values obtained for the PHA.A.2.3.1.1 fibres. As shown in Table 2, the PHA.A.2.3.1.1 fibre exhibited the highest crystallinity, which corresponded to the lowest elongation values.

For the blended fibres, the inclusion of PHA.C.3.3.1.4 significantly improved their elongation properties due to its exceptional elongation characteristics. Specifically, elongation increased from 18 ± 180.4% (for neat PHBHHX fibres) and 0.9 ± 43.7% (for neat PHA.A.2.3.1.1 fibres) to 74 ± 98.1% and 10 ± 144.7%, respectively, in blends containing PHA.C.3.3.1.4. These values are consistent with those obtained in previous analyses, further supporting the idea that blending enhances properties by promoting strong bond formation between the polymers.

**Table 3.** Data relevant to thermal characterization by DSC and TGA analysis (n = 3; S.D. < 1%).

| Properties | PHBHHx | PHA.A.2.3.1.1 | PHA.C.3.3.1.4 | PHA.C.3.3.1.4 / PHBHHx | PHA.C.3.3.1.4 / PHA.A.2.3.1.1 |
|---|---|---|---|---|---|
| **Linear Mass (dtex)** | 1.65±44.9 | 3.96±64.0 | 4.12±57.9 | 1.46±37.7 | 0.96±11.40 |
| **Tenacity (cN/dtex)** | 0.4 | 0.4 | 0.4 | 0.2 | 0.4 |
| **Elongation (%)** | 18±180.4 | 0.9±43.7 | 136±90.5 | 74±98.1 | 10±144.7 |
| **Linear Mass (dtex)** | 1.65±44.9 | 3.96±64.0 | 4.12±57.9 | 1.46±37.7 | 0.96±11.40 |

## 4. Conclusions

Wet spun fibres were successfully produced from different PHAs at a 15% concentration, demonstrating distinct morphological, thermal, and mechanical properties. Morphological analysis revealed that neat PHBHHx fibres exhibited a spongy structure due to phase separation during coagulation, a feature absents in neat PHA.C.3.3.1.4 fibres, which displayed a more uniform and rounded geometry. Blended fibres achieved smaller and more uniform diameters, with the PHA.C.3.3.1.4/PHBHHx blend showing the smallest and most consistent morphology. FTIR analyses

 doi:10.20944/preprints202507.0116.v1



showed characteristics bands in both PHA unprocessed and fibres FTIR spectra. No differences were observed between those different structures, indicating that wet spinning processing does not affect the molecular structure of each polymer.

Thermal analysis indicated that unprocessed PHA polymers were more thermally stable than the wet spun fibres, with PHBHHx identified as the most thermally vulnerable. Blended fibres, however, exhibited enhanced miscibility and efficient chain alignment, reflected in higher crystallinity, and melting temperatures compared to neat fibres. Mechanical testing further highlighted the superior elongation at break of neat PHA.C.3.3.1.4 fibres, likely due to improved polymer chain entanglements and stronger inter-polymer bonding.

The findings also highlight the impact of low feed rates during extrusion, which can increase fibre amorphousness and introduce processing-induced defects, thereby compromising the thermal stability and mechanical tenacity of the fibres. Therefore, future studies should explore optimized feed rates to improve processing efficiency and fibre quality.

Overall, these results demonstrate the potential of polymer blending to enhance fibre properties through stronger inter-polymer interactions, offering a pathway towards fibres with superior functionality and broader application potential.

**Supplementary Materials:** The following supporting information can be downloaded at the website of this paper posted on Preprints.org, Figure S1. Distribution of individual diameters of wet-spun fibres; Figure S2. Distribution of diameters of individual fibres; Table S1. Descriptive analyses of each PHA individual fibres produced; Table S2. Statistical significance of the diameter distribution among various PHA wet-spun fibre formulations.

**Author Contributions:** Conceptualization, M.A.T. and C.G.; methodology, M.A.T. and C.G.; validation, H.V., C.G. and C.S.; formal analysis, C.S.; investigation, M.A.T.; I.L.; R.G.; writing—original draft preparation, M.A.T.; writing—review and editing, H.V. and C.G.; supervision, H.V., C.G. and C.S.; project administration, H.V. All authors have read and agreed to the published version of the manuscript.

**Funding:** This work was carried out under the Waste2BioComp project - Converting organic waste into sustainable bio-based components, GA 101058654, funded under the topic HORI-ZON-CL4-2021-TWIN-TRANSITION-01-05 of the Horizon Europe 2021 – 2027 programme.

**Data Availability Statement:** The original contributions presented in this study are included in the article/Supplementary Materials. Further inquiries can be directed to the corresponding authors.

**Acknowledgments:** This work was carried out under the Waste2BioComp project - Converting organic waste into sustainable bio-based components, GA 101058654, funded under the topic HORI-ZON-CL4-2021-TWIN-TRANSITION-01-05 of the Horizon Europe 2021 – 2027 programme.

**Conflicts of Interest:** The authors declare no conflicts of interest.

## References

1. Nayanathara Thathsarani Pilapitiya, P.G.C.; Ratnayake, A.S. The World of Plastic Waste: A Review. *Cleaner Materials* 2024, *11*, 100220, doi:10.1016/j.clema.2024.100220.
2. Atiwesh, G.; Mikhael, A.; Parrish, C.C.; Banoub, J.; Le, T.A.T. Environmental Impact of Bioplastic Use: A Review. *Heliyon* 2021, *7*, e07918, doi:10.1016/j.heliyon.2021.e07918.
3. Kumar, R.; Lalnundiki, V.; Shelare, S.D.; Abhishek, G.J.; Sharma, S.; Sharma, D.; Kumar, A.; Abbas, M. An Investigation of the Environmental Implications of Bioplastics: Recent Advancements on the Development of Environmentally Friendly Bioplastics Solutions. *Environ Res* 2024, *244*, 117707, doi:10.1016/j.envres.2023.117707.
4. Research, G.V. Bioplastics Market Size, Share & Trends Analysis Report By Product (Biodegradable, Non-Biodegradable), By Application, By Region, And Segment Forecasts; 2023;
5. Rosenboom, J.G.; Langer, R.; Traverso, G. Bioplastics for a Circular Economy. *Nat Rev Mater* 2022, *7*, 117–137, doi:10.1038/s41578-021-00407-8.

 doi:10.20944/preprints202507.0116.v1




6. Zhao, X.; Wang, Y.; Chen, X.; Yu, X.; Li, W.; Zhang, S.; Meng, X.; Zhao, Z.-M.; Dong, T.; Anderson, A.; et al. Sustainable Bioplastics Derived from Renewable Natural Resources for Food Packaging. *Matter* 2023, *6*, 97–127, doi:10.1016/j.matt.2022.11.006.
7. Vanheusden, Chris; Vanminsel, Jan; Reddy, Naveen; Ethirajan, Anitha;Buntinx, M. Fabrication of Poly(3-Hydroxybutyrate-Co-3-Hydroxyhexanoate) Fibers Using Centrifugal Fiber Spinning: Structure, Properties and Application Potential. *Polymers (Basel)* 2023, *15*.
8. Siracusa, Valentina and Blanco, I. Polymers Analogous to Petroleum-Derived Ones for Packaging and Engineering Applications. *Polymers (Basel)* 2020, *12*, 1641.
9. Ali, S.S.; Abdelkarim, E.A.; Elsamahy, T.; Al-Tohamy, R.; Li, F.; Kornaros, M.; Zuorro, A.; Zhu, D.; Sun, J. Bioplastic Production in Terms of Life Cycle Assessment: A State-of-the-Art Review. *Environmental Science and Ecotechnology* 2023, *15*, 100254, doi:10.1016/j.ese.2023.100254.
10. Behera, S.; Priyadarshanee, M.; Vandana; Das, S. Polyhydroxyalkanoates, the Bioplastics of Microbial Origin: Properties, Biochemical Synthesis, and Their Applications. *Chemosphere* 2022, *294*, 133723, doi:10.1016/j.chemosphere.2022.133723.
11. Kaniuk, Ł.; Stachewicz, U. Development and Advantages of Biodegradable PHA Polymers Based on Electrospun PHBV Fibers for Tissue Engineering and Other Biomedical Applications. *ACS Biomater Sci Eng* 2021, *7*, 5339–5362, doi:10.1021/acsbiomaterials.1c00757.
12. Sanhueza, C.; Acevedo, F.; Rocha, S.; Villegas, P.; Seeger, M.; Navia, R. Polyhydroxyalkanoates as Biomaterial for Electrospun Scaffolds. *Int J Biol Macromol* 2019, *124*, 102–110, doi:10.1016/j.ijbiomac.2018.11.068.
13. Naser, A.Z.; Deiab, I.; Darras, B.M. Poly(Lactic Acid) (PLA) and Polyhydroxyalkanoates (PHAs), Green Alternatives to Petroleum-Based Plastics: A Review. *RSC Adv* 2021, *11*, 17151–17196, doi:10.1039/D1RA02390J.
14. Madison, L.L.; Huisman, G.W. Metabolic Engineering of Poly(3-Hydroxyalkanoates): From DNA to Plastic. *Microbiology and Molecular Biology Reviews* 1999, *63*, 21–53, doi:10.1128/MMBR.63.1.21-53.1999.
15. Hu, D.; Chung, A.-L.; Wu, L.-P.; Zhang, X.; Wu, Q.; Chen, J.-C.; Chen, G.-Q. Biosynthesis and Characterization of Polyhydroxyalkanoate Block Copolymer P3HB- b -P4HB. *Biomacromolecules* 2011, *12*, 3166–3173, doi:10.1021/bm200660k.
16. Choi, S.Y.; Cho, I.J.; Lee, Y.; Kim, Y.; Kim, K.; Lee, S.Y. Microbial Polyhydroxyalkanoates and Nonnatural Polyesters. *Advanced Materials* 2020, *32*, doi:10.1002/adma.201907138.
17. Garcia-Garcia, D.; Fenollar, O.; Fombuena, V.; Lopez-Martinez, J.; Balart, R. Improvement of Mechanical Ductile Properties of Poly(3-Hydroxybutyrate) by Using Vegetable Oil Derivatives. *Macromol Mater Eng* 2017, *302*, 1600330, doi:10.1002/mame.201600330.
18. Tan, D.; Wang, Y.; Tong, Y.; Chen, G.-Q. Grand Challenges for Industrializing Polyhydroxyalkanoates (PHAs). *Trends Biotechnol* 2021, *39*, 953–963, doi:10.1016/j.tibtech.2020.11.010.
19. McAdam, B.; Brennan Fournet, M.; McDonald, P.; Mojicevic, M. Production of Polyhydroxybutyrate (PHB) and Factors Impacting Its Chemical and Mechanical Characteristics. *Polymers (Basel)* 2020, *12*, 2908, doi:10.3390/polym12122908.
20. Tang, H.J.; Neoh, S.Z.; Sudesh, K. A Review on Poly(3-Hydroxybutyrate-Co-3-Hydroxyhexanoate) [P(3HB-Co-3HHx)] and Genetic Modifications That Affect Its Production. *Front Bioeng Biotechnol* 2022, *10*, doi:10.3389/fbioe.2022.1057067.
21. Rai, R.; Keshavarz, T.; Roether, J.A.; Boccaccini, A.R.; Roy, I. Medium Chain Length Polyhydroxyalkanoates, Promising New Biomedical Materials for the Future. *Materials Science and Engineering: R: Reports* 2011, *72*, 29–47, doi:10.1016/j.mser.2010.11.002.
22. Tang, H.J.; Neoh, S.Z.; Sudesh, K. A Review on Poly(3-Hydroxybutyrate-Co-3-Hydroxyhexanoate) [P(3HB-Co-3HHx)] and Genetic Modifications That Affect Its Production. *Front Bioeng Biotechnol* 2022, *10*, doi:10.3389/fbioe.2022.1057067.
23. Uddin, Md.K.; Novembre, L.; Greco, A.; Sannino, A. Polyhydroxyalkanoates, A Prospective Solution in the Textile Industry - A Review. *Polym Degrad Stab* 2024, *219*, 110619, doi:10.1016/j.polymdegradstab.2023.110619.

 doi:10.20944/preprints202507.0116.v1




24. Miranda, C.S.; Marinho, E.; Seabra, C.L.; Evenou, C.; Lamartine, J.; Fromy, B.; Costa, S.P.G.; Homem, N.C.; Felgueiras, H.P. Antimicrobial, Antioxidant and Cytocompatible Coaxial Wet-Spun Fibers Made of Polycaprolactone and Cellulose Acetate Loaded with Essential Oils for Wound Care. *Int J Biol Macromol* 2024, *277*, 134565, doi:10.1016/j.ijbiomac.2024.134565.
25. Miranda, C.S.; Silva, A.F.G.; Pereira-Lima, S.M.M.A.; Costa, S.P.G.; Homem, N.C.; Felgueiras, H.P. Tunable Spun Fiber Constructs in Biomedicine: Influence of Processing Parameters in the Fibers' Architecture. *Pharmaceutics* 2022, *14*, 164, doi:10.3390/pharmaceutics14010164.
26. Kopf, S.; Åkesson, D.; Skrifvars, M. Textile Fiber Production of Biopolymers – A Review of Spinning Techniques for Polyhydroxyalkanoates in Biomedical Applications. *Polymer Reviews* 2023, *63*, 200–245, doi:10.1080/15583724.2022.2076693.
27. Kundrat, V.; Matouskova, P.; Marova, I. Facile Preparation of Porous Microfiber from Poly-3-(R)-Hydroxybutyrate and Its Application. *Materials* 2019, *13*, 86, doi:10.3390/ma13010086.
28. Singhi, B.; Ford, E.N.; King, M.W. The Effect of Wet Spinning Conditions on the Structure and Properties of Poly-4-hydroxybutyrate Fibers. *J Biomed Mater Res B Appl Biomater* 2021, *109*, 982–989, doi:10.1002/jbm.b.34763.
29. Degeratu, C.N.; Mabilleau, G.; Aguado, E.; Mallet, R.; Chappard, D.; Cincu, C.; Stancu, I.C. Polyhydroxyalkanoate (PHBV) Fibers Obtained by a Wet Spinning Method: Good in Vitro Cytocompatibility but Absence of in Vivo Biocompatibility When Used as a Bone Graft. *Morphologie* 2019, *103*, 94–102, doi:10.1016/j.morpho.2019.02.003.
30. Alagoz, A.S.; Rodriguez-Cabello, J.C.; Hasirci, V. PHBV Wet-Spun Scaffold Coated with ELR-REDV Improves Vascularization for Bone Tissue Engineering. *Biomedical Materials* 2018, *13*, 055010, doi:10.1088/1748-605X/aad139.
31. Puppi, D.; Pirosa, A.; Morelli, A.; Chiellini, F. Design, Fabrication and Characterization of Tailored Poly[(R)-3-Hydroxybutyrate-Co-(R)-3-Hydroxyexanoate] Scaffolds by Computer-Aided Wet-Spinning. *Rapid Prototyp J* 2018, *24*, 1–8, doi:10.1108/RPJ-03-2016-0037.
32. Gao, C.; He, S.; Qiu, L.; Wang, M.; Gao, J.; Gao, Q. Continuous Dry–Wet Spinning of White, Stretchable, and Conductive Fibers of Poly(3-Hydroxybutyrate- Co -4-Hydroxybutyrate) and ATO@TiO 2 Nanoparticles for Wearable e-Textiles. *J Mater Chem C Mater* 2020, *8*, 8362–8367, doi:10.1039/D0TC01310B.
33. Puppi, D.; Morelli, A.; Chiellini, F. Additive Manufacturing of Poly(3-Hydroxybutyrate-Co-3-Hydroxyhexanoate)/Poly(ε-Caprolactone) Blend Scaffolds for Tissue Engineering. *Bioengineering* 2017, *4*, 49, doi:10.3390/bioengineering4020049.
34. Miranda, C.S.; Silva, A.F.G.; Seabra, C.L.; Reis, S.; Silva, M.M.P.; Pereira-Lima, S.M.M.A.; Costa, S.P.G.; Homem, N.C.; Felgueiras, H.P. Sodium Alginate/Polycaprolactone Co-Axial Wet-Spun Microfibers Modified with N-Carboxymethyl Chitosan and the Peptide AAPV for Staphylococcus Aureus and Human Neutrophil Elastase Inhibition in Potential Chronic Wound Scenarios. *Biomaterials Advances* 2023, *151*, 213488, doi:10.1016/j.bioadv.2023.213488.
35. Puppi, D.; Chiellini, F. Wet-Spinning of Biomedical Polymers: From Single-Fibre Production to Additive Manufacturing of Three-Dimensional Scaffolds. *Polym Int* 2017, *66*, 1690–1696, doi:10.1002/pi.5332.
36. Abdulrahman, A.; van Walsum, G.P.; Um, B.-H. Acetic Acid Removal from Pre-Pulping Wood Extract with Recovery and Recycling of Extraction Solvents. *Appl Biochem Biotechnol* 2019, *187*, 378–395, doi:10.1007/s12010-018-2826-z.
37. Watkins, P. Comparing the Use of Chloroform to Petroleum Ether for Soxhlet Extraction of Fat in Meat. *Anim Prod Sci* 2023, *63*, 1445–1449, doi:10.1071/AN23014.
38. Puppi, D.; Pirosa, A.; Morelli, A.; Chiellini, F. Design, Fabrication and Characterization of Tailored Poly[(R)-3-Hydroxybutyrate-Co-(R)-3-Hydroxyexanoate] Scaffolds by Computer-Aided Wet-Spinning. *Rapid Prototyp J* 2018, *24*, 1–8, doi:10.1108/RPJ-03-2016-0037.
39. Yan, J.; Zhou, G.; Knight, D.P.; Shao, Z.; Chen, X. Wet-Spinning of Regenerated Silk Fiber from Aqueous Silk Fibroin Solution: Discussion of Spinning Parameters. *Biomacromolecules* 2010, *11*, 1–5, doi:10.1021/bm900840h.

 doi:10.20944/preprints202507.0116.v1




40. Han, W.; Wang, L.; Li, Q.; Ma, B.; He, C.; Guo, X.; Nie, J.; Ma, G. A Review: Current Status and Emerging Developments on Natural Polymer-Based Electrospun Fibers. *Macromol Rapid Commun* 2022, *43*, doi:10.1002/marc.202200456.
41. Mota, C.; Wang, S.-Y.; Puppi, D.; Gazzarri, M.; Migone, C.; Chiellini, F.; Chen, G.-Q.; Chiellini, E. Additive Manufacturing of Poly[( R )-3-Hydroxybutyrate- Co -( R )-3-Hydroxyhexanoate] Scaffolds for Engineered Bone Development. *J Tissue Eng Regen Med* 2017, *11*, 175–186, doi:10.1002/term.1897.
42. Chen, L.; Pan, D.; He, H. Morphology Development of Polymer Blend Fibers along Spinning Line. *Fibers* 2019, *7*, 35, doi:10.3390/fib7040035.
43. Zakaria, M.; Shibahara, K.; Nakane, K. Melt-Electrospun Polyethylene Nanofiber Obtained from Polyethylene/Polyvinyl Butyral Blend Film. *Polymers (Basel)* 2020, *12*, 457, doi:10.3390/polym12020457.
44. Lu, H.; Kazarian, S.G.; Sato, H. Simultaneous Visualization of Phase Separation and Crystallization in PHB/PLLA Blends with In Situ ATR-FTIR Spectroscopic Imaging. *Macromolecules* 2020, *53*, 9074–9085, doi:10.1021/acs.macromol.0c00713.
45. Trakunjae, C.; Boondaeng, A.; Apiwatanapiwat, W.; Kosugi, A.; Arai, T.; Sudesh, K.; Vaithanomsat, P. Enhanced Polyhydroxybutyrate (PHB) Production by Newly Isolated Rare Actinomycetes Rhodococcus Sp. Strain BSRT1-1 Using Response Surface Methodology. *Sci Rep* 2021, *11*, 1896, doi:10.1038/s41598-021-81386-2.
46. Ramezani, M.; Amoozegar, M.A.; Ventosa, A. Screening and Comparative Assay of Poly-Hydroxyalkanoates Produced by Bacteria Isolated from the Gavkhooni Wetland in Iran and Evaluation of Poly-β-Hydroxybutyrate Production by Halotolerant Bacterium Oceanimonas Sp. GK1. *Ann Microbiol* 2015, *65*, 517–526, doi:10.1007/s13213-014-0887-y.
47. Otaru, A.J.; Alhulaybi, Z.A.; Dubdub, I. Machine Learning Backpropagation Prediction and Analysis of the Thermal Degradation of Poly (Vinyl Alcohol). *Polymers (Basel)* 2024, *16*, 437, doi:10.3390/polym16030437.
48. Dehouche, N.; Idres, C.; Kaci, M.; Zembouai, I.; Bruzaud, S. Effects of Various Surface Treatments on Aloe Vera Fibers Used as Reinforcement in Poly(3-Hydroxybutyrate-Co-3-Hydroxyhexanoate) (PHBHHx) Biocomposites. *Polym Degrad Stab* 2020, *175*, 109131, doi:10.1016/j.polymdegradstab.2020.109131.
49. Berrabah, I.; Dehouche, N.; Kaci, M.; Bruzaud, S.; Deguines, C.H.; Delaite, C. Morphological, Crystallinity and Thermal Stability Characterization of Poly(3-Hydroxybutyrate-Co-3-Hydroxyhexanoate)/Zinc Oxide Nanoparticles Bionanocomposites: Effect of Filler Content. *Mater Today Proc* 2022, *53*, 223–227, doi:10.1016/j.matpr.2022.01.032.
50. Vanheusden, C.; Samyn, P.; Goderis, B.; Hamid, M.; Reddy, N.; Ethirajan, A.; Peeters, R.; Buntinx, M. Extrusion and Injection Molding of Poly(3-Hydroxybutyrate-Co-3-Hydroxyhexanoate) (PHBHHx): Influence of Processing Conditions on Mechanical Properties and Microstructure. *Polymers (Basel)* 2021, *13*, 4012, doi:10.3390/polym13224012.
51. Díez-Pascual, A.; Díez-Vicente, A. Poly(3-Hydroxybutyrate)/ZnO Bionanocomposites with Improved Mechanical, Barrier and Antibacterial Properties. *Int J Mol Sci* 2014, *15*, 10950–10973, doi:10.3390/ijms150610950.
52. Di Lorenzo, M.L.; Androsch, R. Crystallization of Poly[(R)-3-Hydroxybutyrate]. In; 2019; pp. 119–142.
53. Vahabi, H.; Michely, L.; Moradkhani, G.; Akbari, V.; Cochez, M.; Vagner, C.; Renard, E.; Saeb, M.R.; Langlois, V. Thermal Stability and Flammability Behavior of Poly(3-Hydroxybutyrate) (PHB) Based Composites. *Materials* 2019, *12*, 2239, doi:10.3390/ma12142239.
54. Xie, R.; Weisen, A.R.; Lee, Y.; Aplan, M.A.; Fenton, A.M.; Masucci, A.E.; Kempe, F.; Sommer, M.; Pester, C.W.; Colby, R.H.; et al. Glass Transition Temperature from the Chemical Structure of Conjugated Polymers. *Nat Commun* 2020, *11*, 893, doi:10.1038/s41467-020-14656-8.
55. Seymour, R.B.; Carraher, C.E. Mechanical Properties of Polymers. In *Structure—Property Relationships in Polymers*; Springer US: Boston, MA, 1984; pp. 57–72.
56. Puchalski, M.; Kwolek, S.; Szparaga, G.; Chrzanowski, M.; Krucińska, I. Investigation of the Influence of PLA Molecular Structure on the Crystalline Forms (α′ and α) and Mechanical Properties of Wet Spinning Fibres. *Polymers (Basel)* 2017, *9*, 18, doi:10.3390/polym9010018.

 doi:10.20944/preprints202507.0116.v1




57. Asim, M.; Paridah, M.T.; Chandrasekar, M.; Shahroze, R.M.; Jawaid, M.; Nasir, M.; Siakeng, R. Thermal Stability of Natural Fibers and Their Polymer Composites. *Iranian Polymer Journal* 2020, *29*, 625–648, doi:10.1007/s13726-020-00824-6.
58. Singhi, B.; Ford, E.N.; King, M.W. The Effect of Wet Spinning Conditions on the Structure and Properties of Poly-4-hydroxybutyrate Fibers. *J Biomed Mater Res B Appl Biomater* 2021, *109*, 982–989, doi:10.1002/jbm.b.34763.
59. Park, S.; Park, J.K. Back to Basics: The Coagulation Pathway. *Blood Res* 2024, *59*, 35, doi:10.1007/s44313-024-00040-8.
60. Mirbaha, H.; Scardi, P.; D'Incau, M.; Arbab, S.; Nourpanah, P.; Pugno, N.M. Supramolecular Structure and Mechanical Properties of Wet-Spun Polyacrylonitrile/Carbon Nanotube Composite Fibers Influenced by Stretching Forces. *Front Mater* 2020, *7*, doi:10.3389/fmats.2020.00226.
61. Pereira, C.; Pinto, T. V.; Santos, R.M.; Correia, N. Sustainable and Naturally Derived Wet Spun Fibers: A Systematic Literature Review. *Fibers* 2024, *12*, 75, doi:10.3390/fib12090075.
62. Consul, P.; Beuerlein, K.-U.; Luzha, G.; Drechsler, K. Effect of Extrusion Parameters on Short Fiber Alignment in Fused Filament Fabrication. *Polymers (Basel)* 2021, *13*, 2443, doi:10.3390/polym13152443.
63. Pecorini, G.; Braccini, S.; Simoni, S.; Corti, A.; Parrini, G.; Puppi, D. Additive Manufacturing of Wet-Spun Poly(3-hydroxybutyrate- Co -3-hydroxyvalerate)-Based Scaffolds Loaded with Hydroxyapatite. *Macromol Biosci* 2024, *24*, doi:10.1002/mabi.202300538.
64. Kim, J.; Zhang, G.; Shi, M.; Suo, Z. Fracture, Fatigue, and Friction of Polymers in Which Entanglements Greatly Outnumber Cross-Links. *Science (1979)* 2021, *374*, 212–216, doi:10.1126/science.abg6320.
65. Feijoo, P.; Samaniego-Aguilar, K.; Sánchez-Safont, E.; Torres-Giner, S.; Lagaron, J.M.; Gamez-Perez, J.; Cabedo, L. Development and Characterization of Fully Renewable and Biodegradable Polyhydroxyalkanoate Blends with Improved Thermoformability. *Polymers (Basel)* 2022, *14*, 2527, doi:10.3390/polym14132527.